

## Experimental Investigations on the Stagnation Behavior of Thermochromic Flat Plate Collectors

Sebastian Müller<sup>1</sup>, Rolf Reineke-Koch<sup>1</sup>, Federico Giovannetti<sup>1</sup>, Bernd Hafner<sup>2</sup>

<sup>1</sup> Institut für Solarenergieforschung Hameln (ISFH), Am Ohrberg 1, D-31860 Emmerthal (Germany),  
Phone: +49 5151 999-646, E-Mail: mueller@isfh.de

<sup>2</sup> Viessmann Werke GmbH & Co. KG, Viessmannstraße 1, D-35108 Allendorf (Germany)

### Abstract

A thermochromic absorber coating in a solar thermal flat plate collector switches its emissivity for thermal radiation depending on the absorber temperature. Thus, the stagnation temperature can be reduced by 30 K compared to a standard flat plate collector and an overheating of the heat transfer fluid can be prevented. On the basis of 58 selected stagnation events we analyze and compare the stagnation behavior of solar thermal systems with standard and thermochromic collectors. We have carried out well defined stagnation experiments to determine the steam expansion, steam volume and steam producing power for the two solar thermal systems with unfavorable system hydraulics. By the use of thermochromic collectors at a standard system overpressure (1.0 bar) the steam expansion can be halved, the overall steam volume can be lowered by 33 % and the stagnation time can be reduced by 20 %. The steam expansion and the vaporization of the heat transfer fluid can be prevented at system overpressures above 3.4 bar and 4.1 bar, respectively. The steam producing power can be limited to 40 W·m<sup>-2</sup>.

*Keywords: thermochromic absorber coating, flat plate collector, stagnation behavior, stagnation load*

---

## 1. Introduction

The stagnation temperature of standard flat plate collectors with a highly selective absorber coating (absorptance  $\alpha \geq 95$  %, emittance  $\varepsilon \approx 5$  %) can easily reach up to 200 °C. Especially in summer, with high solar irradiance and low domestic hot water demand, the downtime of the solar pump increases. In case of stagnation, high thermal loads occur both in systems for solar domestic hot water (SDHW) preparation and solar assisted space heating. A stagnation event is usually accompanied with the vaporization of the heat transfer fluid in the collector array. The steam replaces the fluid in the collector and can spread vastly into the solar piping. The temperature stress can damage sensitive solar loop components (e.g. pumps, membrane expansion vessel, insulation material, valves). To protect these components, temperature resistant materials or additional devices have to be installed to withstand the stagnation load. Furthermore, high system temperatures induce a faster degradation of the heat transfer fluid as reported in Scheuren et al. (2006). This results in higher investment, installation and maintenance costs.

The stagnation loads can be reduced significantly by preventing the vaporization of the heat transfer fluid. Scheuren and Kirchner (2008a) investigated the stagnation behavior in detail and characterized different collector types on the basis of their steam producing power. To prevent overheating and handle the stagnation loads, Harrison et al. (2012) and Frank et al. (2015) summarized different protective arrangements and stagnation control strategies. Föste et al. (2016a) and Schiebler et al. (2018a) developed different types of heat pipe collectors which can reduce the thermal stagnation loads by avoiding the vaporization of the heat transfer fluid. Drainback solar thermal systems can prevent the vaporization in the solar loop as well, as reported by Botpaev et al. (2016). To reduce the stagnation loads in flat plate collectors, Brunold et al. (2007) suggested the use of thermochromic layers (based on vanadium oxides) and Föste et al. (2016b) investigated industrially manufactured thermochromic flat plate collectors. First stagnation experiments with these kind of collectors were carried out by Müller et al. (2017).

Thermochromic absorber coatings have a highly temperature dependent emissivity for thermal radiation. Above a predetermined “switching point” (ca. 68 °C absorber temperature) its emittance increases from 5 % up to 35 %. This process is due to a semiconductor-to-metal transition of the active absorber layer, is fully reversible and increases the thermal heat losses significantly. Thus, the stagnation temperature can be reduced by 30 K compared to a standard flat plate collector. Despite slightly worse optical properties at the present development stage, the high performance of thermochromic flat plate collectors in a SDHW system was confirmed by Müller et al. (2017) by means of dynamic system testing according to ISO 9459-5.

This paper presents and discusses the experimental results concerning the stagnation behavior of thermochromic flat plate collectors in a SDHW system with a collector area of 10 m<sup>2</sup>, focusing on the steam expansion, steam volume, steam producing power and the stagnation dynamics.

## 2. Process of stagnation

The downtime of the pump in a solar thermal system despite high solar irradiance is called stagnation. Usually, this operating condition occurs, if the storage tank reaches its cut-off temperature. Stagnation has to be considered as a conventional operating condition during the planning and dimensioning of a SDHW system. However, fatal system errors, like a damaged solar pump, leakages of the piping or a blackout, can effect stagnation too. In this case, the solar irradiance on the collector after solar pump shutdown is still converted into thermal energy, which cannot be transferred to the solar loop. Once the absorber temperature  $T_{Abs}$  exceeds the saturation temperature  $T_S$  of the heat transfer fluid at a given system pressure, the fluid starts to vaporize and steam replaces the collector fluid content. The steam spreads into the solar piping and the collector outlet temperatures  $T_{FL}$  and  $T_{RL}$  rise abruptly while the system overpressure  $p_{Coll}$  at the collector outlet reaches a maximum. The remaining liquid vaporizes quickly during the stagnation event and overheated steam can expand into the solar piping. With decreasing irradiance the steam condensates gradually and backs down to the collector. This general stagnation behavior is shown in Fig. 1.

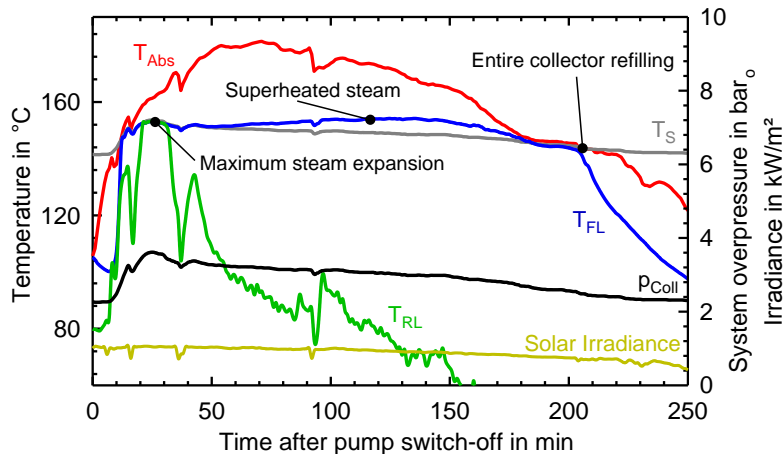


Fig. 1: Typical temporal progression of the system overpressure ( $p_{Coll}$ ), the absorber temperature ( $T_{Abs}$ ) and the temperatures of the collectors' in- and outlet ( $T_{FL}$ ,  $T_{RL}$ ) after pump shutdown.

The stagnation process in a solar thermal collector array can be described by characteristic parameters, like the steam expansion into the solar piping, the steam producing power, the system steam volume and the remaining fluid volume within the collector array. These are important indicators for a proper dimensioning of the membrane expansion vessel (MEV) and additional cooling components. They depend on the collector efficiency at stagnation and on the hydraulic design.

### 2.1 Steam expansion

The temporal progression of steam expansion ( $SE$ ) can be detected by the use of temperature sensors mounted directly onto the stainless steel corrugated solar piping (cf. Fig. 3.b). We identify the steam expansion in the piping by temperature sensors placed at discrete positions  $s$ . The temperature detected between two nodes  $s_n$  and  $s_{n+1}$  is compared to the saturation temperature  $T_S$ . If the expansion front is located in between these nodes, the distance is averaged accord to eq. 1, both for flow (FL) and return line (RL). The overall steam expansion  $SE$  is the sum of the two single steam expansions (cf. eq. 2).

$$SE_{FL/RL} = \frac{1}{2} \cdot (s_n + s_{n+1}) \quad (\text{eq. 1})$$

$$SE = SE_{FL} + SE_{RL} \quad (\text{eq. 2})$$

The uncertainty of this measurement method depends primarily on the distance between two temperature sensors and is equal or lower than  $\pm 0.87$  m for  $SE$ . The saturation temperature  $T_S$  of the used heat transfer fluid Tyfocor LS (60 vol% water, 40 vol% propylene glycol) depends on the *absolute* system pressure at the geodetic height of the collector array  $p_{\text{Coll,a}}$ . According to the manufacturers' datasheet,  $T_S$  can be calculated approximately as

$$T_S = 100 \text{ °C} + 35.1 \text{ K} \cdot \ln(p_{\text{Coll,a}}). \quad (\text{eq. 3})$$

## 2.2 Steam producing power

Scheuren et al. (2006) assumed that the thermal losses of the insulated pipe are equal to the steam producing power ( $SPP$ ) of the collector array at the moment of maximum  $SE$ , so that  $SPP$  [ $\text{W} \cdot \text{m}^{-2}$ ] can be calculated as

$$SPP = \frac{SE \cdot \dot{q}_{\text{Loss,Pipe}}}{n_{\text{Coll}} \cdot A_{\text{Coll,Ap}}}. \quad (\text{eq. 4})$$

The length-specific thermal losses of the solar piping  $\dot{q}_{\text{Loss,Pipe}}$  have been measured in preliminary tests for fluid temperatures up to 105 °C. The results were quadratically fitted in terms of the temperature difference of the fluid temperature  $T_{\text{Fluid}}$  and the collector ambient temperature  $T_{\text{ca}}$  (cf. eq. 5). In case of a stagnation event,  $T_{\text{Fluid}}$  is assumed equal to the saturation temperature  $T_S$ .

$$\dot{q}_{\text{Loss,Pipe}} = 0.23604 \frac{\text{W}}{\text{m} \cdot \text{K}} \cdot (T_{\text{Fluid}} - T_{\text{ca}}) + 0.00046 \frac{\text{W}}{\text{m} \cdot \text{K}^2} \cdot (T_{\text{Fluid}} - T_{\text{ca}})^2 \quad (\text{eq. 5})$$

Based on several stagnation experiments, Scheuren and Kirchner (2008a) developed a model for  $SPP$  as a function of the collector efficiency parameters ( $\eta_0$ ,  $a_1$  and  $a_2$ ), environmental conditions (effective irradiance  $G_{\text{Stag}}$ , ambient temperature  $T_{\text{ca}}$ ) and the system pressure (through the saturation temperature  $T_S$ , cf. eq. 3). Their model assumes, that the temperature of the absorber plate and the steam is equal to the saturation temperature  $T_S$ . At maximum  $SE$  a quantity referred to as “theoretical collector performance during stagnation”  $P_{\text{Stag}}$  is calculated according to

$$P_{\text{Stag}} = G_{\text{Stag}} \cdot \eta_0 - a_1 \cdot (T_S - T_{\text{ca}}) - a_2 \cdot (T_S - T_{\text{ca}})^2. \quad (\text{eq. 6})$$

From their investigations the authors derived three different collector classes with good (A), moderate (B) and bad (C) draining behavior, which are characterized by increasing  $SPP$ .

## 2.3 System steam volume

The overall system steam volume ( $SV$ ) can be used for both dimensioning the MEV and evaluating the draining behavior of the system. During a stagnation event the replaced collector fluid is received by the MEV and thus, the system pressure increases. The overall system steam volume  $SV$  may be referred to the net expansion volume  $V_{\text{exp}}$  of the MEV according to

$$SV = V_{\text{exp,max}} - V_{\text{exp,0}} \quad (\text{eq. 7})$$

where  $V_{\text{exp,0}}$  and  $V_{\text{exp,max}}$  are the volumes at the beginning of the stagnation event and at maximum steam expansion, respectively. This methodology was introduced by Scheuren (2008b). For each MEV the expansion volume as a function of the system overpressure has to be determined in a calibration test bed. The calibration curves for three different pre-set pressures are displayed in Fig. 2. Two MEV specific parameters, the nominal volume  $V_N$  and the MEV constant  $c_{\text{MEV}}$ , are determined during the calibration process as well. The expansion volume  $V_{\text{exp}}$  can then be calculated with the measured *absolute* system pressure  $p_{\text{MAG,a}}$  at the MEV inlet according to eq. 8.

$$V_{\text{exp}} = V_N - c_{\text{MAG}} \cdot \left( \frac{T_{\text{MEV}}}{p_{\text{MEV,a}}} \right) \quad (\text{eq. 8})$$

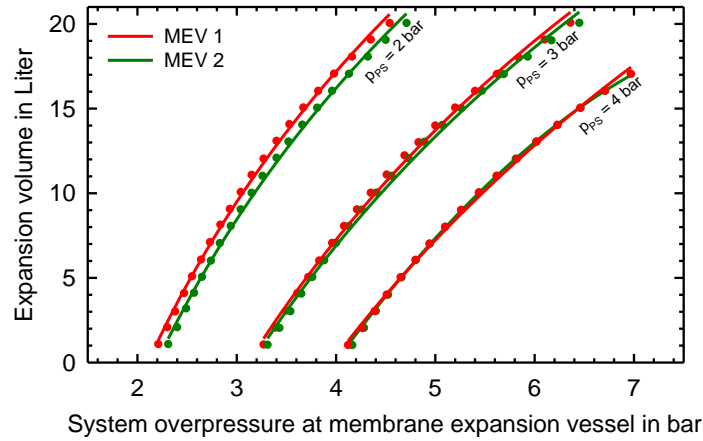


**Fig. 2: Expansion volume of both calibrated MEVs with a nominal volume of 50 liters as a function of the system overpressure for three different MEV pre-set pressures.**

The nominal volumes of the identically manufactured MEV are  $V_{N,MEV1} = 46.6$  liters and  $V_{N,MEV2} = 46.5$  liters. The two MEV constants also depend on the *absolute* pre-set pressure  $p_{ps,a}$  and can be calculated as

$$c_{MEV1} = 0.1460 \cdot p_{ps,a} - 0.067 \text{ and} \quad (\text{eq. 9})$$

$$c_{MEV2} = 0.1325 \cdot p_{ps,a} - 0.120.$$

Following Scheuren (2008b), this calibration method exhibits an uncertainty for the determination of  $V_{Exp}$  for low and high fluid inlet temperatures  $T_{MEV}$  of 5 % and 10 %, respectively.

#### 2.4 Remaining liquid within the collector

After the collector draining a significant volume of heat transfer fluid can remain in the collector. This remaining fluid volume (*RFV*) consists of concentrated propylene glycol, which exhibits a higher boiling temperature than water. The amount of *RFV* depends significantly on the draining behavior of the collector array. *RFV* is calculated indirectly from the system steam volume *SV* and the steam expansion *SE* as

$$RFV = n_{Coll} \cdot V'_{Coll} + SE \cdot V'_{Pipe} - SV. \quad (\text{eq. 10})$$

The installed corrugated stainless steel piping has a length-specific fluid volume  $V'_{Pipe} = 0.27$  liters per meter (DN 16). The collector fluid content  $V'_{Coll} = 1.80$  liters per collector. In both of our systems  $n_{Coll} = 4$  collectors are installed. According to Scheuren (2008b), the calculation of the *RFV* exhibits a large uncertainty of approximately 30 %. Especially in the wave troughs of corrugated pipes a not definable amount of fluid can remain. Thus, the real *RFV* in the collector is always lower than the calculated value according to eq. 10.

### 3. Experimental investigations on the stagnation behavior

Föste et al. (2016b) predicted by means of simulations, that a thermochromic SDHW system could lower the stagnation time (here: timespan, during which the absorber temperature is above 120 °C) by more than 70 %. To verify their simulative results, we have carried out extensive stagnation tests on real systems under natural environmental conditions.

#### 3.1 Experimental setting

Two identical SDHW systems were installed on an outdoor testing roof at ISFH: A thermochromic system and a reference system with standard flat plate collectors (see Fig. 3.a). Each collector array consists of four flat plate collectors with a gross area of 10 m<sup>2</sup>. The solar piping of both systems feature identical designs, so as to guarantee the same thermohydraulic behavior. The overall length of the solar piping is 30 m for each system, installed bottom-up the roof, which can be considered as a worst-case scenario. Hence, the measured steam expansion and steam volume can be considered as maximum values for this hydraulic configuration.

We installed temperature sensors (Pt1000) in the wave trough of the corrugated stainless steel piping, starting from the collector in- and outlet in regular intervals of 1.5 meters, to determine the steam expansion according

to eq. 1. The temperature distribution in the collector array is measured at the absorber plate of each collector. In addition, we installed sensors at thermal sensitive components, like the MEV or the solar pump. One pressure sensor was added at the collector array outlet to investigate the stagnation dynamics and possible hydraulic shocks. All sensors and their positions are displayed in the hydraulic schema of Fig. 3.b.

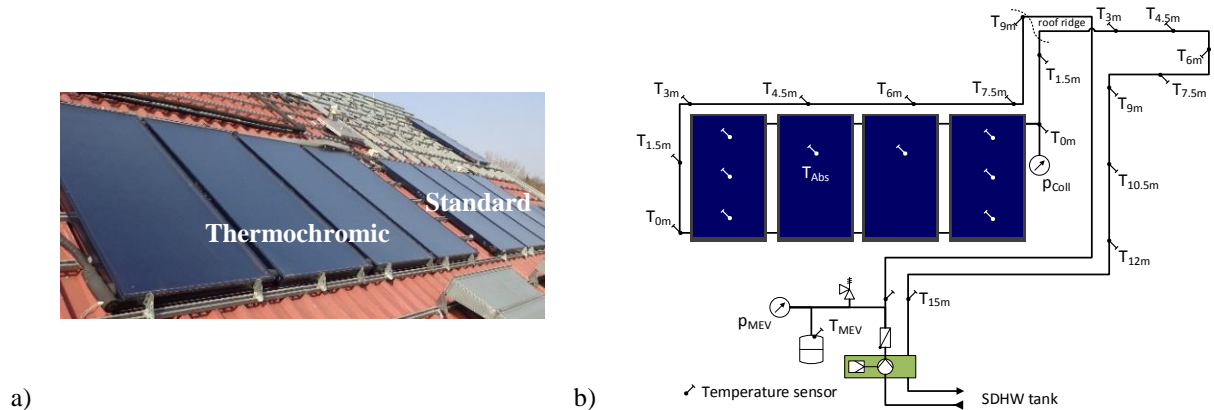


**Fig. 3: Standard and thermochromic SDHW systems installed on our outdoor testing roof to evaluate the stagnation loads (a) and positions of the sensors used in our investigations (b).**

We performed several stagnation tests by operating the two systems synchronously to directly compare their stagnation behavior. The stagnation events were carried out in the evaluation period from 20.06. – 21.10.2017 and 03.04. – 02.07.2018 (212 days, 4.898 hours of data) under natural environmental weather conditions with a great variability of the ambient temperature  $T_{ca}$  (16.6...37.0 °C) and the effective solar irradiance  $G_{Stag}$  (800...1150 W·m<sup>-2</sup>) at the beginning of a stagnation event. We operated both SDHW systems on four different resting overpressures measured at the geodetic height of the collector outlet (cf. Fig. 3.b) between 1.0 and 4.0 bar. This pressure is referred to as “system overpressure” in the sequel.

### 3.2 Methodology of evaluation

The experiments can be distinguished into two characteristic stagnation types: full-time stagnation and noon stagnation. At a full-time stagnation the solar pump remains deactivated throughout the day, which results in an early stagnation start. Hence, the stagnation time and the maximum thermal loads of the heat transfer fluid can be determined. At a noon stagnation the solar pump is switched off manually at solar noon (circa 12:00...12:30PM). Both stagnation types are presented in Fig. 4. During the considered experimental period we have recorded 58 stagnation events, 34 of them as noon and 24 as full-time stagnation experiments.

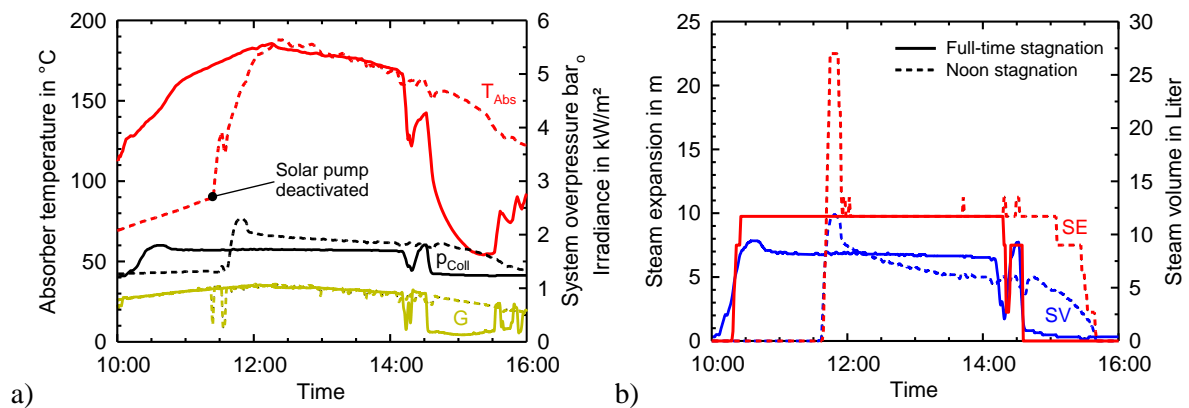


**Fig. 4: Absorber temperature  $T_{Abs}$  and overpressure at collector height  $p_{Coll}$  (a) as well as steam expansion  $SE$  and steam volume  $SV$  (b) of thermochromic and standard system in comparison for different stagnation types. The slashed and the solid curves are related to a noon stagnation and a full-time stagnation, respectively.**

The maximum absorber temperature  $T_{Abs}$  is independent from the stagnation type and reaches in both cases 190 °C for a standard flat plate collector. During a full-time stagnation the vaporization starts typically at approximately 10 AM, indicated by the increase of the system overpressure  $p_{Coll}$  from 1.2 bar to 1.8 bar. In contrast, for a noon stagnation experiment we detected overpressures up to 2.3 bar (see Fig. 4.a). The collector

efficiency at the beginning of the stagnation event is an important indicator for the *SE*. Due to high solar irradiance, the collector efficiency for a noon stagnation is higher than for a full-time stagnation and results in an *SE* of 23 m. If the vaporization starts early in the morning, the *SE* does not exceed 11 m in our experiments (see Fig. 4.b).

## 4. Evaluation of stagnation events

### 4.1 Thermal loads

We define the stagnation time  $t_{stag}$  as the timespan between beginning vaporization of the heat transfer fluid and full re-condensation of any steam in the system. At a standard system overpressure of 1.0 bar,  $t_{stag}$  can be reduced with thermochromic collectors by 20 % and at 3.0 bar up to 60 %. The measured temperature and steam expansion distributions as detected for four system overpressures are displayed in Fig. 5 for noon stagnations.

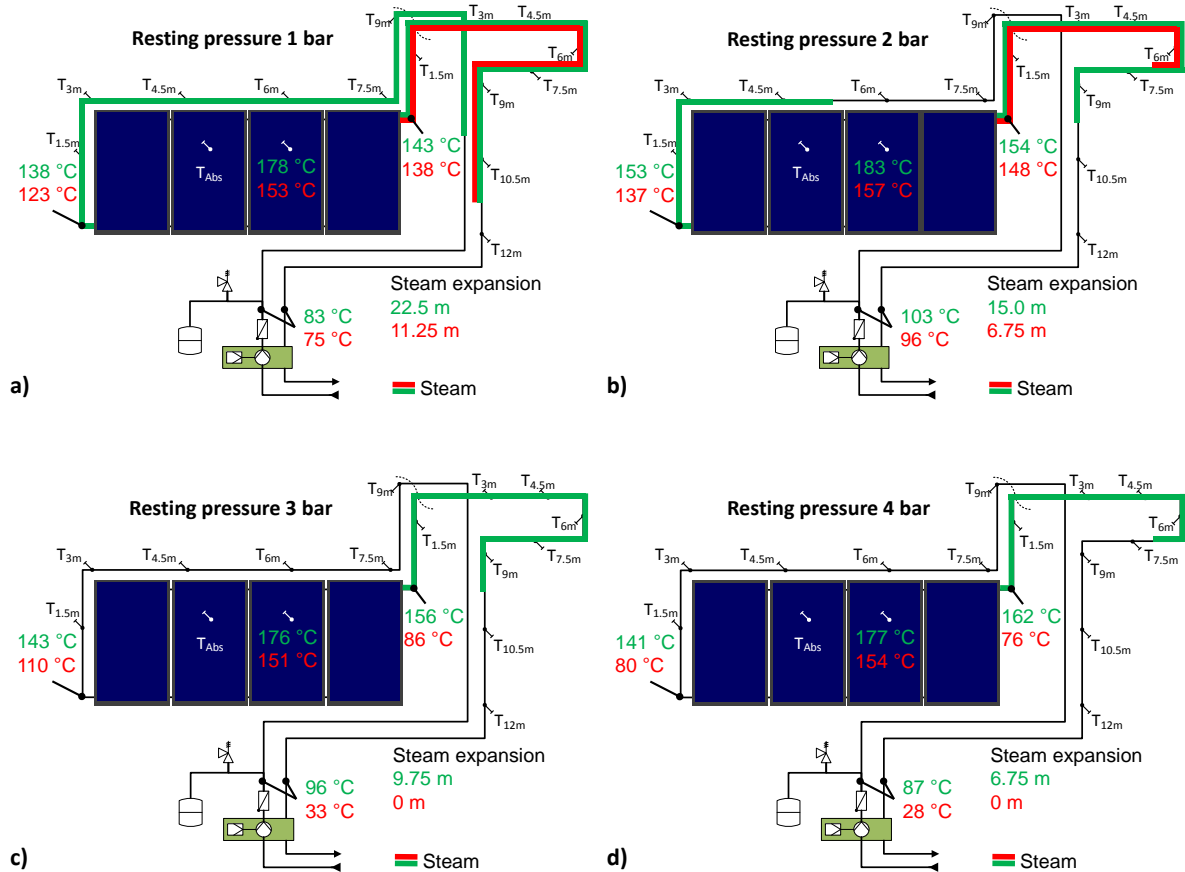


Fig. 5: Temperature distribution and steam expansion in both SDHW systems for four representative noon stagnation events. (green values: standard collector, red values: thermochromic)

At a system overpressure of 1.0 bar, the absorber temperature exceeds easily the current saturation temperature (ca. 125 °C) and the heat transfer fluid vaporizes. In the reference system with standard collectors and in the system with thermochromic collectors we detect a steam expansion of 22.5 m and 11.3 m, respectively (see Fig. 5.a). The installed temperature sensors allow a time-resolved analysis of the draining behavior. In both SDHW systems the heat transfer fluid is draining through the return line in case of vaporization and thereupon the steam expands only in the flow line at first. The steam spreads into the upper section of the piping up to the geodetic height of the collector array inlet and not till then into the return line as well. In the thermochromic system we can only detect a steam expansion into the flow line due to a permanently refilling of the collector array over the return line. We can report a reduction of the maximum absorber temperature of thermochromic collectors up to 25 K compared to standard flat plate collectors. Due to the length of the solar piping the steam never expands to sensitive system components. Nevertheless, hot fluid may reach the solar pump station or the MEV. At a system overpressure of 2.0 bar temperatures of 100 °C were detected at the solar pump station (see Fig. 5.b). In contrast, for the thermochromic system at elevated system overpressure the temperature does not

exceed 35 °C. If the steam expansion can be prevented, the maximum collector outlet temperature in the thermochromic system decreases to 86 °C compared to 156 °C for standard flat plate collectors (see Fig. 5.c) and the inlet temperatures can be reduced to 110 °C. At a system overpressure of 4.0 bar any vaporization in the thermochromic system can be prevented (see Fig. 5.d). Thus, the collector array in- and outlet temperatures do not exceed 80 °C compared to 160 °C in the standard system.

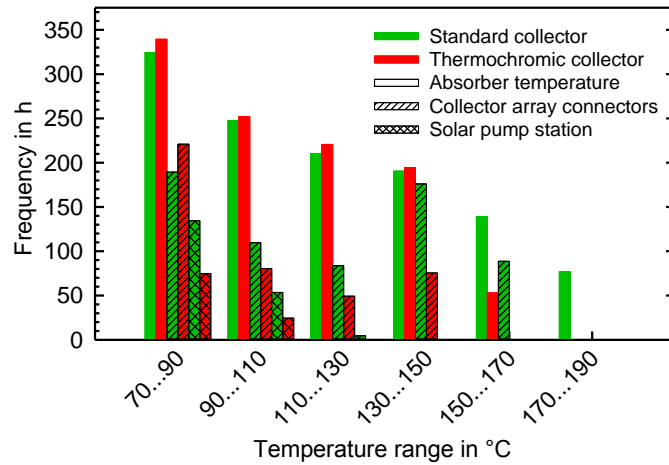


Fig. 6: Frequency distribution of several system temperatures occurred during the evaluation period for the standard (green) and the thermo-chromic (red) SDHW system.

We provide the frequency distributions of the observed temperatures in Fig. 6. We report maximum absorber temperatures in the thermo-chromic and standard system up to 164 °C and 191 °C, respectively. For a total time of 77 hours temperatures above 170 °C occurred in the standard system, which exceeds the design temperature of the heat transfer fluid. High thermal loads lead to a thermal decomposition of the propylene glycol, which can strongly reduce its lifetime and can impair the reliability of the whole system. The temperature at the collector array connectors (maximum in- and outlet temperature) during stagnation is primarily defined by the saturation temperature  $T_S$  due to steam expansion into the solar piping. Maximum temperatures of 150 °C and 167 °C can be measured for the thermo-chromic and the standard SDHW system, respectively. According to the manufacturer, the design temperature of the solar pump station is 110 °C. Maximum temperatures directly in front of the solar pump station higher than 120 °C temporarily occur in both systems. We measured for a total time of 0.8 hours and 4.8 hours temperatures higher than 110 °C in the thermo-chromic and the standard SDHW system, respectively. Especially at low system overpressures of 1...2 bar, a noon stagnation results in a high steam expansion and thus high temperatures at the solar pump station.

#### 4.2 Steam expansion

The maximum steam expansion ( $SE$ ) have generally been observed for noon stagnation experiments. The measured  $SE$  for both systems is plotted against the system overpressure in Fig. 7. At 1.0 bar a noon stagnation results for the standard and the thermo-chromic system in a  $SE$  of 22.5 m and 11.3 m respectively. The steam expansion is halved for thermo-chromic collectors at this specific system overpressure. Above a system overpressure of 3.4 bar, the steam expansion into the solar piping is suppressed for the thermo-chromic system. In the standard system we still measure a steam expansion of 10 m. For full-time stagnations, the  $SE$  in the thermo-chromic system is generally 40...50 % lower than in the reference system.

The great variability of measured  $SE$  for one specific system overpressure results on the one hand on the different environmental weather conditions (cf. Fig. 8.a) and on the other hand on noon-stagnation events, which were temporarily interrupted by clouds while steam expansion.



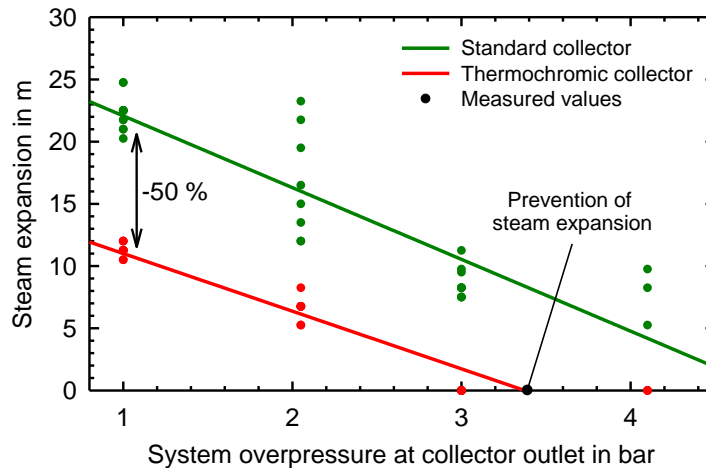


Fig. 7: Steam expansion as a function of the system overpressure at the collector outlet for all measured noon stagnations.

### 4.3 Steam producing power

The resulting *SPP* are shown in Fig. 8.a as a function of the effective solar irradiance  $G_{\text{Stag}}$ . We employ linear regressions to emphasize the trend progression. Inspection shows that for the standard collector under full-time stagnation conditions the *SPP* is 55 % lower than under noon stagnation conditions. For thermochromic collectors the *SPP* is limited to approximately  $40 \text{ W}\cdot\text{m}^{-2}$ . The mean *SPP* for different system overpressures are represented in Fig. 8.b. We see that at a system overpressure of 1.0 bar the mean *SPP* is  $77 \text{ W}\cdot\text{m}^{-2}$  and  $37 \text{ W}\cdot\text{m}^{-2}$  for standard and thermochromic collectors, respectively. Similar results are reported for a system overpressure of 2.0 bar. We conclude that the *SPP* of the studied systems is reduced by about 50 % with thermochromic compared to standard collectors. Note that for system overpressures above 3 bar no steam expansion occurs in the thermochromic system, due to the high saturation temperature of the heat transfer fluid (cf. Fig. 7). The error bars characterize a variability of the results of up to  $\pm 15 \text{ W}\cdot\text{m}^{-2}$ .

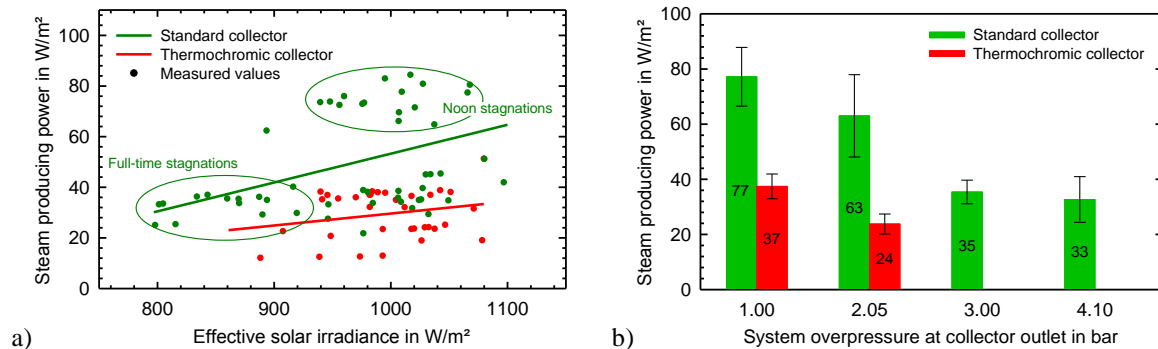


Fig. 8: Steam producing power as a function of the effective solar irradiance for all measured stagnation events (a) and mean *SPP* plotted against the system overpressure at collector outlet just for noon stagnations (b). The error bars represent the standard deviation of the calculated mean *SPP*.

The theoretical collector performance of all experiments are evaluated according to the model of Scheuren and Kirchner (2008a) (cf. eq. 6, see Fig. 9). Again, linear regressions are used to visualize trend behavior. The plots confirm that the *SPP* increases with the theoretical collector performance, as expected. According to their classification the standard system may be categorized as Class B, which corresponds to a system with flat plate collectors and unfavorable draining behavior in the author's original work. The thermochromic system exhibits under identical hydraulic conditions lower *SPP* and may be classified between Class A and B, according to this scheme. We conclude that an increase of  $P_{\text{Stag}}$  in the thermochromic system results in lower *SPP* compared to the standard system.



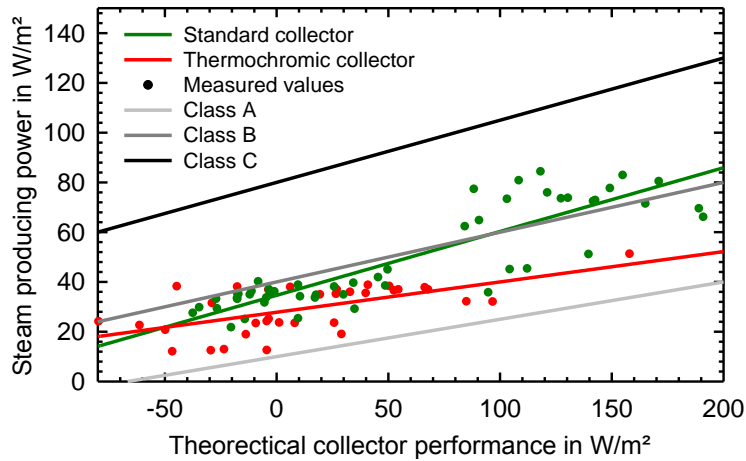


Fig. 9: Steam producing power as a function of the theoretical collector performance for all measured stagnation events.

Note that for negative theoretical collector performances both collector arrays produce a significant amount of steam, which is basically related to the model assumption, that the mean collector (absorber and fluid) temperature is equal to the saturation temperature  $T_s$  (cf. eq. 6). For collectors with unfavorable draining behavior this assumption might often not be valid, because a great amount of remaining fluid volume could significantly reduce the average collector temperature.

#### 4.4 Steam volume and remaining fluid

The overall system steam volume, which we determine with the calibrated MEVs (cf. eq. 7), is shown as a function of the system overpressure in Fig. 10. For system overpressures of 1.0 bar,  $SV$  can be reduced by 33 % with thermochromic collectors. For 2.0 bar,  $SV$  can be halved compared to standard collectors. Although we could not measure a  $SE$  for a system pressure above 3.0 bar, a certain amount of 2 liters can be detected within the thermochromic system. The steam does not expand into the solar piping and only remains within the collector array. Based on the physical properties of the heat transfer fluid and the occurring temperatures, the vaporization can be prevented above system overpressures of 4.1 bar (stagnation temperature 157 °C) for thermochromic collectors, whereas 9.6 bar would be necessary for standard collectors (183 °C). Such a high system overpressure clearly exceeds the components acceptable operating conditions.

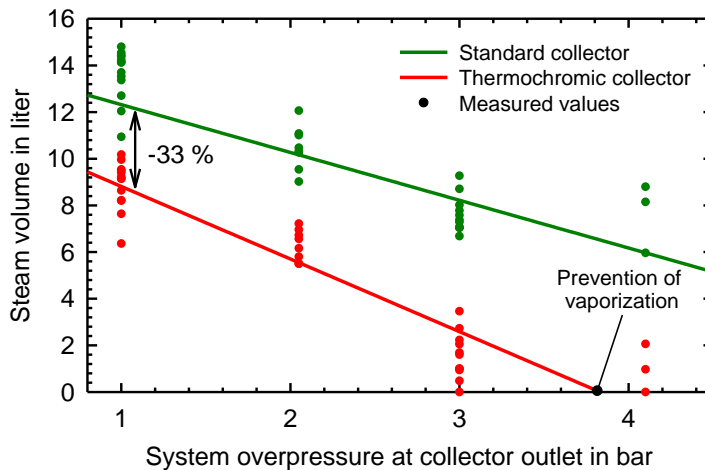


Fig. 10: Steam expansion as a function of the system overpressure at collector outlet for noon stagnations.

The remaining fluid volume ( $RFV$ ) was calculated for all selected noon stagnations according to eq. 10 and is plotted in Fig. 11. Generally, the  $RFV$  depends on the system overpressure. With rising system overpressure the collector efficiency and thus, the steam volume and steam expansion decreases, while the mean  $RFV$  increases. We could determine mean  $RFVs$  at standard system overpressure (1.0 bar) of 0.4 and 1.4 liters for the standard and thermochromic system, respectively. At 2.0 bar the mean  $RFVs$  increase to 1.4 and 2.7 liters and at 3.0 bar to 1.8 and 5.5 liters. The measured steam expansion at a specific system overpressure is almost independent from the  $RFV$ . In our investigation a large number of measured  $RFVs$  can result in the same steam expansion. In

the thermochromic system for example at a system overpressure of 1.0 bar we measured *RFVs* between 0.1 and 4.1 liters, which correspond to measured steam expansions between 10.5 and 12 m.

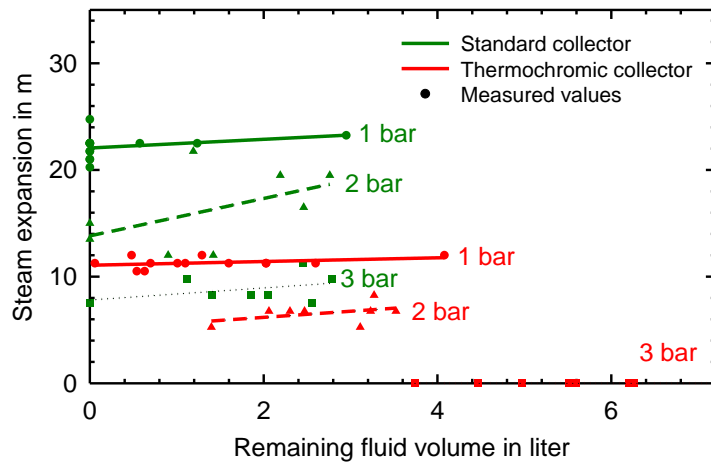


Fig. 11: Steam expansion as a function of the remaining fluid volume at various system overpressures for noon stagnations.

We can determine only a marginal increase of steam expansion for higher values of *RFV* (linear regressions in Fig. 11). At low *RFVs* the collector piping is extensively filled with steam and the heat transfer between the absorber plate and the heat transfer fluid is inhibited. Hence, the collector efficiency decreases and the steam expansion is accordingly lower. Furthermore, the collector array hydraulics and the connection of the solar piping are significantly responsible for the amount of *RFV*.

## 5. Conclusions and outlook

We experimentally investigated the stagnation behavior of thermochromic flat plate collectors in a solar thermal domestic hot water system by analyzing several stagnation events in detail. For our tests we installed two collector arrays consisting of four standard and four thermochromic collectors respectively, with an overall gross area of 10 m<sup>2</sup> each. The two systems were operated synchronously under the same environmental conditions. We identified and evaluated important system parameters, like the steam expansion, the overall system steam volume and the remaining fluid volume in the collector.

On the basis of 58 selected stagnation events at four different system overpressures, we report a significant reduction of the thermal loads in the thermochromic system in case of stagnation compared to the standard system. The maximum absorber temperature can be reduced up to 30 K, which confirms our previous laboratory results (Föste et al., 2016b). At a system overpressure of 1.0 bar the steam expansion into the solar piping can be halved from 22.5 m to 11.3 m and the overall system steam volume can be reduced by 33 %. At a system overpressure of 2.0 bar the thermal loads are significantly lower: By the use of thermochromic collectors both the stagnation time (here: timespan, in which any steam occurs in the system) and the steam volume can be halved. At a system overpressure of 3.4 bar the steam expansion in the thermochromic system can be prevented. Hence, the temperature at the collector in- and outlet can be limited to 110 °C and reduced by 70 K. At system overpressures above 4.1 bar the vaporization of the heat transfer fluid can be avoided. For the standard system this state is expected above 9.6 bar, i.e. for pressure conditions which solar components are not designed for.

We conclude, that the use of thermochromic collectors in a commonly dimensioned solar thermal system operating under standard conditions can significantly reduce the temperature occurring in the case of stagnation. By slightly increasing the system pressure, the vaporization can be completely suppressed and thus, the thermal load in the whole system can be reduced. This offers a great potential for a substantial reduction of the specific system costs for investment, installation (e.g. use of plastics for the solar piping or avoidance of additional measures like cooling devices) and maintenance (e.g. longer lifetime of the heat transfer fluid) as reported by Schiebler et al. (2018b).

## Acknowledgement

This investigations were carried out in the frame of the project “Process technology, quality assessment and system solutions for thermochromic absorbers in solar thermal collectors (ProTASK)”, which is funded by the German Federal Ministry of Economic Affairs and Energy based on a decision of the German Federal Parliament (reference numbers 0325858 A and B). The project ProTASK is carried out in cooperation with Viessmann Werke GmbH & Co. KG.

The authors are grateful for the financial support and responsible for the paper’s content.

## References

- Botpaev, R., Louvet, Y., Perers, B., Furbo, S., Vajen, K., 2016. Drainback solar thermal systems: A review. *Solar Energy* 128, pp. 41 – 60. DOI: 10.1016/j.solener.2015.10.050.
- Frank, E., Mauthner, F., Fischer, S., 2015. Overheating prevention and stagnation handling in solar process heat applications. IEA SHC Task 49, Technical Report A.1.2.
- Föste, S., Schiebler, B., Giovannetti, F., Rockendorf, G., Jack, S., 2016. Butane heat pipes for stagnations temperature reduction of solar thermal collectors. *Energy Procedia* 91, pp. 35 – 41. DOI: 10.1016/j.egypro.2016.06.168.
- Föste, S., Pazidis, A., Reineke-Koch, R., Hafner, B., Mercks, D., Delord, C., 2016. Flat plate collectors with thermochromic absorber coatings to reduce loads during stagnation. *Energy Procedia* 91, pp. 42 – 48. DOI: 10.1016/j.egypro.2016.06.169.
- Harrison, S., Cruickshank, C. A., 2012. A review of strategies for the control of high temperature stagnation in solar collectors and systems. *Energy Procedia* 30, pp. 793 – 804. DOI: 10.1016/j.egypro.2012.11.090.
- ISO 9459-5, 2007. System performance characterization by means of whole-system tests and computer simulation. Beuth Verlag, Berlin.
- Müller, S., Reineke-Koch, R., Giovannetti, F., Hafner, B., 2017. Flat Plate Collectors with Thermochromic Absorber Coating Under Dynamic System Tests. *Proceedings ISES Solar World Congress 2017*, pp. 2062 - 2070, Abu Dhabi. DOI: 10.18086/swc.2017.31.10.
- Scheuren, J., Kirchner, M., Eisenmann, W., 2006. Reduction of Stagnation Load of Large-Scale Collector Arrays. *Proceedings EuroSun 2006*, International Solar Energy Society (ISES), Freiburg.
- Scheuren, J., Kirchner, 2008. Analysis and Prediction of the Steam-Producing Power in Large-Scale Collector Arrays under Stagnation Conditions. *Proceedings EuroSun 2008*, International Solar Energy Society (ISES), Freiburg.
- Scheuren, J., 2008. Untersuchung zum Stagnationsverhalten solarthermischer Kollektorfelder. Kassel University Press.
- Schiebler, B., Jack, S., Dieckmann, H., Giovannetti, F., 2018. Experimental and theoretical investigations on temperature limitation in solar thermal collectors with heat pipes: Effect of superheating on the maximum temperature, *Solar Energy* 171, 271 - 278. DOI: 10.1016/j.solener.2018.06.036.
- Schiebler, B., Giovannetti, F., Fischer, S., 2018: Levelized cost of heat of solar domestic hot water systems with overheating prevention, IEA SHC TASK 54, Info Sheet B5.